

# Two methods to approximate the superposition of imperfect failure processes

Shaomin Wu

*Kent Business School, University of Kent, Canterbury, Kent CT2 7FS, United Kingdom*

email: [s.m.wu@kent.ac.uk](mailto:s.m.wu@kent.ac.uk)

Suggested citation: Wu, S. (2020) Two methods to approximate the superposition of imperfect failure processes, *Reliability Engineering and System Safety*, DOI: [10.1016/j.ress.2020.107332](https://doi.org/10.1016/j.ress.2020.107332)

---

## Abstract

Suppose a series system is composed of a number of repairable components. If a component fails, it is repaired immediately and the effectiveness of the repair may be imperfect. Then the failure process of the component can be modelled by an imperfect failure process and the failure process of the system is the superposition of the failure processes of all components. In the literature, there is a bulk of research on the superimposed renewal process (SRP) for the case where the repair on each component is assumed perfect. For the case that the component causing the system to fail is unknown and that repair on a failed component is imperfect, however, there is little research on modelling the failure process of the system. Typically, the likelihood functions for the superposition of imperfect failure processes cannot be given explicitly. Approximation-based models have to be sought. This paper proposes two methods to model the failure process of a series system in which the failure process of each component is assumed an arithmetic reduction of intensity and an arithmetic reduction of age model, respectively. The likelihood method of parameter estimation is given. Numerical examples and real-world data are used to illustrate the applicability of the proposed models.

*Key words:* Arithmetic reduction of intensity (ARI) model; arithmetic reduction of age (ARA) model; superimposed ARI (SARI) model; superimposed ARA (SARA) model.

---

## 1. Introduction

In the reliability literature, repair effectiveness can be categorised into perfect, imperfect and minimal. Suppose an item failed. A perfect repair on the item is equivalent to replacing the item with a new identical item, that is, it brings the failed item to the good-as-new status; a minimal repair restores the item to the status just before the item failed, namely, it brings the failed item to the bad-as-old status; and an imperfect repair brings the item to a status between the good-as-new and bad-as-old statuses. Usually, the renewal process is used to model the interfailure times of perfect repairs; the non-homogeneous Poisson process is for those of minimal repairs; and models such as the arithmetic reduction of intensity (ARI) model and the arithmetic reduction of age (ARA) model are for those of imperfect repairs [1, 2, 3]. There is a bulk of research discussing different types of stochastic processes for modelling failure processes, or simply put, modelling interfailure times, see [1, 2, 3, 4], for example. These models are also applied in maintenance policy optimisation, see [5, 6, 7, 8, 9, 10, 11, 12], for example.

Consider a system that is composed of multiple components in series. Suppose that the failures of the components are statistically independent. Repair is immediately performed upon a component failure and the repair time is negligible. Suppose the effectiveness of the repair is not minimal.

- If the repair is perfect, then the interfailure times of the system is a superimposed renewal process (SRP). The SRP has received plenty of attention from authors (see [13, 14, 15], for example). The reader is referred to [3] for a recently published paper of SRPs in reliability.
- If the repair effectiveness on the failure of each component is imperfect, the superposition of the imperfect failure processes has not been well investigated in the literature yet.

We refer to the case that the components that cause the system to fail are known and that interfailure time data are available as *unmasked failure data*. With unmasked failure data, if the number of failures of each component is large enough, one may develop a model for the failure process of each component and then aggregate those models to describe the failure process of the system. In the real world, nevertheless, maintenance data may be available in an aggregate form. That is, the interfailure time data are available, but which component causes the system to fail may be unknown. Such data are often referred to as *masked failure data*. In the case of modelling on masked failure data, one is unable to build a model for the failure process of each component and then aggregate them as there is no failure data on each individual component. That is, the superposition of imperfect failure processes (SIRP) cannot be explicitly given. In this case, methods that can approximate the SIRP have to be sought.

Examples of such systems can be found from the real-world. For example, one can regard that a section of pavement is composed of a grid of cells. The section may be regarded failed if there is a large defect such as fatigue cracking on a cell. Maintenance should then be carried out to repair the defect and it is usually imperfect. But when the failure data are analysed, data on which cell causes the section to fail

35 may be unavailable due to various reasons such as a lack of precise location. For the pavement owner, it is  
36 important to have a model of good performance that can estimate the long term costs of maintaining the  
37 pavement. See [16] for other real-world examples. These examples motivate this work.

38 Given a series system composed of multiple components, this paper assumes that the failure process  
39 of each component can be modelled with either the arithmetic reduction of intensity (ARI) model or the  
40 arithmetic reduction of age (ARA) model. The reason that this paper uses the ARI and ARA models  
41 is due to their wide coverage. Some widely studied models, including the model proposed by [17] and  
42 the virtual models proposed by [18, 19], are the special cases of the ARI model and the ARA model,  
43 respectively. This paper proposes methods to approximate the superposition of ARI (SARI) model and  
44 the superposition of ARA (SARA) model, respectively. Probabilistic properties of the proposed methods  
45 are discussed. Artificially generated numerical examples and real-world examples are used to illustrate the  
46 proposed methods. This paper extends the work of [4]. Its managerial implication is that practitioners may  
47 use the proposed methods in their work such as development of maintenance policies and life cycle costing.

48 The remainder of this paper is structured as follows. Section 2 gives assumptions and notations that  
49 are used in the paper. Section 3 investigates the superposition of imperfect failure processes (SIRP) for  
50 the situations when unmasked failure data are available and then gives a method of simulating such an  
51 SIRP. Section 4 proposes methods to approximate the superposition of the ARI process and that of the  
52 ARA process for the case when only masked failure data are available, respectively. Section 5 gives the  
53 likelihood functions of the SARI and the SARA, respectively, and verifies the proposed methods on an  
54 artificially generated dataset and then on a real-world dataset. Section 6 discusses an alternative method to  
55 approximate the SIRP for the case when only truncated failure data are available and also gives the failure  
56 intensity function of the SRP. Section 7 concludes the paper and proposes future research suggestions.

## 57 **2. Assumptions and notations**

58 This section sets notations and assumptions.

### 59 *2.1. Notations*

60 The notations in Table 1 will be used in the paper.

### 61 *2.2. Assumptions*

- 62 • Suppose a series system is composed of  $n$  components, whose interfailure times are statistically inde-  
63 pendent.
- 64 • The failure intensity function of component  $k$  is  $\frac{1}{n}\lambda_k(t)$  before its first failure.
- 65 • Repair is immediately performed upon the failure of a component (or the system). The effectiveness  
66 of repair may be perfect, imperfect, or minimal.

Table 1: Notation Table

---

$n$	number of components
$k$	index of a component in the system, $k = 1, 2, \dots, n$
$t$	time since the system starts, where $t \geq 0$
$N_t$	number of failures of the system up to time $t$
$N_{k,t}$	number of failures of component $k$ up to time $t$
$N$	total number of failures of the system
$i$	index of failures, $i = 1, 2, \dots, N$
$m$	order of memory, where $m \geq 1$ in the $\text{ARI}_m$ model or the $\text{ARA}_m$ model
$j$	index of the order of memory, $j = 1, 2, \dots, \infty$
$\tau$	time since the completion of the latest repair, where $\tau > 0$
$\lfloor x \rfloor$	the largest integer that is smaller than or equal to $x$
$b_{N_t}$	$b_{N_t} = N_t - n \times \lfloor \frac{N_t}{n} \rfloor$ if $N_t \neq n \times \lfloor \frac{N_t}{n} \rfloor$ , $b_{N_t} = n$ otherwise.
$T_{N_t}$	successive failure times of a repairable system; $T_{N_t}$ is a random variable
$T_{k,N_t}$	time to the $i$ th failure of component $k$ after the $N_t$ th repair; $T_{k,N_t}$ is a random variable
$t_{N_t}$	observation of $T_{N_t}$
$t_{k,N_t}$	observation of $T_{k,N_t}$
$\mathcal{H}_{t-}$	history of the failure process up to $t$ (exclusive of $t$ )
$\lambda_k(t)$	failure intensity function of component $k$ if minimal repair is conducted upon failures
$\Lambda_k(t)$	$= \int_0^t \lambda_k(u) du$
$\lambda_{s,k}(t)$	failure intensity function of component $k$ if imperfect repair may be conducted upon failures
$\lambda_s(t)$	failure intensity function of the system at time $t$
$\lambda_s^a(t)$	approximated failure intensity function of the system at time $t$
$h_c(t)$	hazard function of a virtual component at time $t$

---

- 67 • The failure process of a component can be modelled by either the ARI model or the ARA model.
- 68 • The failure process of the system can be defined equivalently by the stochastic processes  $\{T_j\}_{j \geq 1}$  or
- 69  $\{N_t\}_{t \geq 0}$  and is characterised by the intensity function.
- 70 • Although the failure intensity function of an item (which may be a system or a component) should
- 71 be denoted with the memory of  $\mathcal{H}_{t-}$  such as  $\lambda_{s,k}(t|\mathcal{H}_{t-})$  and  $\lambda_s(t|\mathcal{H}_{t-})$ . For the sake of notational
- 72 compactness, this paper will omit the symbol  $\mathcal{H}_{t-}$  and use  $\lambda_{s,k}(t)$  and  $\lambda_s(t)$ , respectively.
- 73 • Repair time is so short that it can be neglected.
- 74 • Only the observations of  $\{T_j\}_{j \geq 1}$  or  $\{N_t\}_{t \geq 0}$  are available, but the source (or component) that causes
- 75 the system to fail is unavailable. Such failure data is hereinafter referred to as masked failure data.

76 **3. Modelling the failure process with unmasked failure data**

77 In this section, we investigate some properties of SARI and SARA, respectively, assuming that the  
78 components that cause the system to fail are known. That is, the failure data are unmasked.

79 *3.1. Related literature on failure process models for multi-component systems*

80 In the literature, there are several papers discussing modelling methods for multi-component systems.  
81 Below we give a brief review on the work published in the last two years. More references in this area can  
82 be found in [2, 4] and [3], respectively.

83 There are many publications methods proposed to approximate the SRP (see [13, 14, 15] for example).  
84 The two following models, Model I and Model II, which were recently proposed in [2].

85 Model I is given by,

86 
$$\lambda_s(t) = h_c(t - T_{N_t}) + \lambda_0(t), \tag{1}$$

87 and Model II is given by,

88 
$$\lambda_s(t) = h_c(t - T_{N_t}) + \frac{1}{n} \left( \sum_{j=0}^{\min\{N_t-1, n-1\}} \lambda_0(t - T_{N_t-j}) + \max\{n - N_t, 0\} \lambda_0(t) \right), \tag{2}$$

89 where  $h_c(t)$  is a hazard function and  $\lambda_0(t)$  is a failure intensity function. Model I in (1) and Model II in (2)  
90 incorporate both time trends (ageing, reliability growth), which is modelled by the first element  $h_c(t - T_{N_t})$ ,  
91 and renewal type behaviour, which is modelled by the second element in the models, respectively.

92 In essence, Model I and Model II integrate two stochastic processes, which requires more parameters  
93 than a single stochastic process. In reality, due to technological advances, today's technical systems have  
94 a small number of failures in their service life. It is therefore difficult to collect a good number of time-to-  
95 failure data (or interfailure time data), based on which the estimated parameters in a failure process model  
96 may have large uncertainty. To reduce the number of parameters, [4] proposes the following model, which  
97 is referred to as *Exponential Smoothing of Intensity* model (ESI), to approximate the SRP.

98 
$$\lambda_s(t) = \frac{1}{n} \sum_{j=0}^{\min\{N_t-1, n-1\}} \rho^{n-j-1} \lambda_0(t - T_{N_t-j}) + \frac{\chi\{1 \leq N_t < n\}}{n} \sum_{j=N_t}^{n-1} \rho^{n-j-1} \lambda_0(t). \tag{3}$$

99 where  $\rho$  is a parameter and  $\rho \in [0, 1]$  and  $\chi\{A\} = 1$  if  $A$  is true,  $\chi\{A\} = 0$  if  $A$  is false. When  $\rho = 1$ , the above  
100 model reduces to a model, which is referred to as the MAI (*Moving Average of Intensity*) model. According  
101 to [4], based on the comparison among ESI and MAI, and nine other existing models on fifteen real-world  
102 datasets, the MAI outperforms the ten other models on eleven datasets (out of the fifteen datasets).

103 Models (1), (2), and (3) are the sum of two intensity functions, which were discussed in the reliability  
104 literature for a different purpose, namely, for modelling bathtub shaped non-monotonic intensities. For  
105 example, [20] assumes the sum of two nonhomogenous Poisson processes with one intensity function being

106 the power law and the other being the log linear law, or both being the power laws [21], or both being the  
 107 log linear laws [22].

108 Models (1), (2), and (3) approximate the SRP (superposition of renewal processes) generated by a multi-  
 109 component system, in which the repair on each component is assumed perfect. In reality, imperfect repair  
 110 occurs from time to time and may be a more realistic measure of maintenance effectiveness. However, in  
 111 the literature, as far as the author's best knowledge, there is little research investigating the superposition  
 112 of imperfect failure processes (SIRP), which motivates the work of the current paper.

113 To model the failure process of a single component, reference [1] investigates several models and cate-  
 114 gorised them into two main classes:  $ARI_m$  (Arithmetic Reduction of Intensity model with memory  $m$ ) and  
 115  $ARA_m$  (Arithmetic Reduction of Age model with memory  $m$  with  $m \geq 1$ ).

116 The  $ARI_m$  model for component  $k$  is given by

$$117 \quad \lambda_{s,k}(t) = \frac{1}{n} \lambda_k(t) - \frac{1}{n} \rho_k \sum_{j=0}^{\min\{m-1, N_t-1\}} (1 - \rho_k)^j \lambda_k(T_{N_t-j}), \quad (4)$$

118 and the  $ARA_m$  model for component  $k$  is given by

$$119 \quad \lambda_{s,k}(t) = \frac{1}{n} \lambda_k \left( t - \rho_k \sum_{j=0}^{\min\{m-1, N_t-1\}} (1 - \rho_k)^j T_{N_t-j} \right). \quad (5)$$

120 where  $\rho_k$  is a parameter representing the repair effectiveness of component  $k$  and  $m$  is the order of the  
 121 memory. That is, Eq. (4) and Eq. (5) assume that the components have different repair effectiveness (i.e.,  
 122  $\rho_k$ ) and the same memory  $m$ .

123 Reference [1] also discuss the cases when  $m = 1$  and  $m = \infty$  for the  $ARI_m$  and the  $ARA_m$  models as  
 124 special cases, respectively.

125 Similar to the methods to approximate the SRP proposed in [2] and [4], we may explore methods to  
 126 approximate the failure process of a system with the failure process of each component modelled by either  
 127  $ARI_m$  or  $ARA_m$ , respectively, as shown in the following section.

### 128 3.2. Superposition of the $ARI_m$ and $ARA_m$ processes, respectively

129 Let's first look at the failure process of a typical system, as shown in Example 1.

130 **Example 1.** Suppose a series system composed of four components, which fail at time points shown in the  
 131 top four horizontal lines in Figure 1. The superposition of the four imperfect failure processes is shown at  
 132 the last horizontal line. In this example, we assume that unmasked failure data are available. If the failure

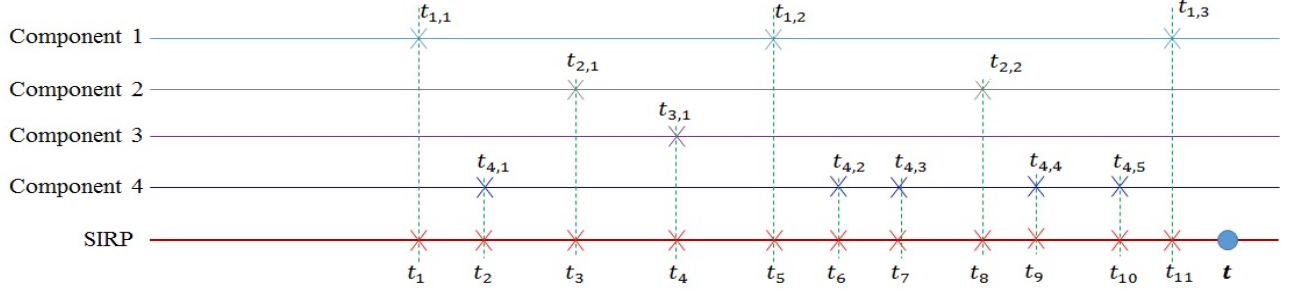


Figure 1: Failure data of a system with four components until time  $t$ , where  $N_{1,t} = 3, N_{2,t} = 2, N_{3,t} = 1$ , and  $N_{4,t} = 5$

133 process of each component is modelled by  $ARI_3$ , then the superposition of the failure processes is given by

$$\begin{aligned}
 134 \quad \lambda_s(t) = & \frac{1}{4} [\lambda_1(t) - \rho_1 \lambda_1(t_{1,3}) - \rho_1(1 - \rho_1) \lambda_1(t_{1,2}) - \rho_1(1 - \rho_1)^2 \lambda_1(t_{1,1}) \\
 135 & + \lambda_2(t) - \rho_2 \lambda_2(t_{2,2}) - \rho_2(1 - \rho_2) \lambda_2(t_{2,1}) \\
 136 & + \lambda_3(t) - \rho_3 \lambda_3(t_{3,1}) \\
 137 & + \lambda_4(t) - \rho_4 \lambda_4(t_{4,5}) - \rho_4(1 - \rho_4) \lambda_4(t_{4,4}) - \rho_4(1 - \rho_4)^2 \lambda_4(t_{4,3})]. \quad (6)
 \end{aligned}$$

139 Similarly, the superposition of the failure processes for the case when the failure process of each compo-  
 140 nent is modelled by  $ARA_3$  can be easily provided.

141 Now suppose that component  $k$  has  $N_{k,t}$  failures that have occurred within  $(0, t)$  and the latest failure  
 142 occurred at time  $T_{k, N_{k,t}}$ . Then the superposition of the  $ARI_m$  processes is given by

$$143 \quad \lambda_s(t) = \frac{1}{n} \sum_{k=1}^n \left( \lambda_k(t) - \sum_{j=0}^{\min\{N_{k,t}-1, m-1\}} \rho_k(1 - \rho_k)^j \lambda_k(T_{k, N_{k,t}-j}) \right). \quad (7)$$

145 The above model is referred to as  $SARI_{n,m}$  (superimposed ARI) in this paper.

146 Similarly, the superposition of failure processes that models the failure process of each component by  
 147 the ARA models, or the  $SARA_{n,m}$  model can be given by

$$148 \quad \lambda_s(t) = \frac{1}{n} \sum_{k=1}^n \lambda_k \left( t - \sum_{j=0}^{\min\{N_{k,t}-1, m-1\}} \rho_k(1 - \rho_k)^j T_{k, N_{k,t}-j} \right). \quad (8)$$

150 According to [23], the  $ARI_m$  model and the  $ARA_m$  model have the asymptotic intensities  $\lambda_{s,k}(t) =$   
 151  $\frac{1}{n}(1 - \rho_k)^m \lambda_k(t)$  and  $\lambda_{s,k}(t) = \frac{1}{n} \lambda_k((1 - \rho_k)^m t)$ , respectively. As such, we can obtain the following Lemma.

152 **Lemma 1.**  $\lambda_s(t)$  in Eq. (7) has the asymptotic intensity  $\frac{1}{n} \sum_{k=1}^n (1 - \rho_k)^m \lambda_k(t)$  and  $\lambda_s(t)$  in Eq. (8) has the

153 asymptotic intensity  $\frac{1}{n} \sum_{k=1}^n \lambda_k((1 - \rho_k)^m t)$ .

154 Lemma 1 implies:  $\lambda_s(t)$  in Eq. (7) (or in Eq. (8)) becomes infinite for  $t \rightarrow \infty$  if  $\lambda_k(t)$  is increasing in  $t$ .  
 155 This result differs from the result of the SRP, on which [24] showed that the SRP tends toward (statistical)  
 156 equilibrium as the time of operation becomes very large.

### 157 3.3. Simulation

158 In the SRP, each failed component in a series system is replaced with a new identical one. As reiterated  
 159 in the preceding paragraph, [24] showed that the SRP tends toward (statistical) equilibrium as the time of  
 160 operation becomes very large, which can be witnessed by viewing numerical examples shown in [3]. It will  
 161 be interesting to see what trends  $SARI_{n,m}$  and  $SARA_{n,m}$  possess as the time of operation becomes very  
 162 large. To this end, this subsection aims to use the Monte Carlo simulation to show their trends.

163 It is noted that  $P(T_{i+1} \leq t_{i+1} | T_i = t_i) = \frac{F(t_{i+1}) - F(t_i)}{1 - F(t_i)} = 1 - \exp(-\Lambda(t_{i+1}) + \Lambda(t_i))$ .

164 Suppose a series system is composed of  $n$  components, which are identical when the system start at  
 165  $t = 0$ . Without loss of generality, let  $\lambda_1(t)$  be the failure intensity function of a component in the system.

166 Then  $\Lambda_1(t) = \int_0^t \lambda_1(u) du$ .

167 The probability of the working time of a given component, component 1, for example, after the  $i$ -th  
 168 repair is given by

- 169 •  $P(T_{1,1} \leq t_{1,1} | T_{1,0} = 0) = 1 - \exp(-\Lambda_1(t_{1,1}))$ ,
- 170 • when the  $ARI_m$  model is used, for  $i \geq 1$ , we have

$$\begin{aligned}
 & P(T_{1,i+1} \leq t_{1,i+1} | T_{1,i} = t_{1,i}, \dots, T_{1,i-\min\{m-1,i-1\}} = t_{1,i-\min\{m-1,i-1\}}) \\
 & = 1 - \exp \left( -\Lambda_1(t_{1,i+1}) + \rho_1 \sum_{j=0}^{\min\{m-1,i-1\}} (1 - \rho_1)^j \lambda_1(t_{1,i-j}) t_{1,i+1} \right. \\
 & \quad \left. + \Lambda_1(t_{1,i}) - \rho_1 \sum_{j=0}^{\min\{m-1,i-1\}} (1 - \rho_1)^j \lambda_1(t_{1,i-j}) t_i \right) \tag{9}
 \end{aligned}$$

- 175 • when the  $ARA_m$  model is used, for  $i \geq 1$ , we have

$$\begin{aligned}
 & P(T_{1,i+1} \leq t_{1,i+1} | T_{1,i} = t_{1,i}, \dots, T_{1,i-\min\{m-1,i-1\}} = t_{1,i-\min\{m-1,i-1\}}) \\
 & = 1 - \exp \left[ -\Lambda_1 \left( t_{1,i+1} - \rho_1 \sum_{j=0}^{\min\{m-1,i-1\}} (1 - \rho_1)^j t_{1,i-j} \right) \right. \\
 & \quad \left. + \Lambda_1 \left( t_{1,i} - \rho_1 \sum_{j=0}^{\min\{m-1,i-1\}} (1 - \rho_1)^j t_{1,i-j} \right) \right]. \tag{10}
 \end{aligned}$$

180 Based on the above discussion, with the Monte Carlo simulation, we can simulate the failure process of a  
 181 system based on a given failure intensity function,  $\lambda_1(t)$ . For example, if we let  $\Lambda_1(t) = \int_0^t \lambda_1(u) du = (\frac{t}{10})^{2.0}$

182 in the SARI model and  $\Lambda_1(t) = \int_0^t \lambda_1(u)du = (\frac{t}{10})^\beta$  in the SARA model,  $\rho_1 = 0.5$ ,  $m = 2$ . Set the number  
 183  $n$  of components in a series system to be 5, 50, 100, and 200, respectively, and their numbers of failures  
 184 are assumed to be  $100 \times n$ , then the failure process according to the failure intensity function given in Eq.  
 185 (7) and that given in Eq. (8) are shown in Fig. 2 for the SARI $_{n,m}$  model and Fig 3 for the SARA $_{n,m}$   
 186 model, respectively. To gain a better understanding, in Fig 3, for the different settings of  $n$ 's and the  
 187 numbers of failures, we also show the cases for  $\beta = 1.5, 2$ , and  $2.5$ , respectively, which are displayed in each  
 188 message box. In the figures, we have divided the entire failure period into 101 units. For example, if the  
 189 time to the 20,000th failure is  $x$ , then we calculate the number of failures in intervals  $(\frac{kx}{101}, \frac{(k+1)x}{101})$  with  
 190  $k = 0, 1, \dots, 101$ , and show the number of failures on the Y-axis and the X-axis shows the 101 units.

191 Fig. 2 and Fig. 3 show that the systems do not develop toward (statistical) equilibrium as the time of  
 192 operation becomes very large. Instead, they become infinity, which agrees with Lemma 1.

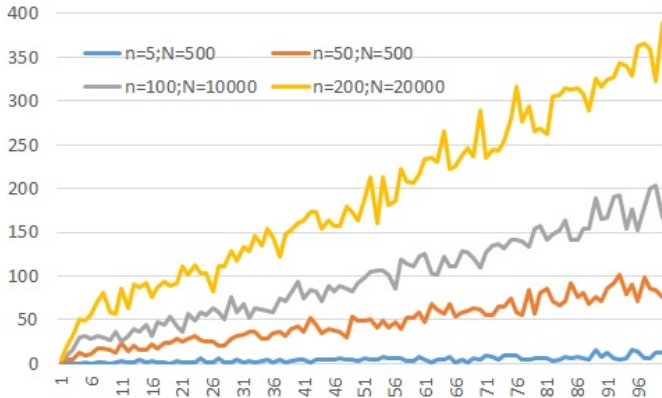


Figure 2:  $\rho_1 = 0.5, m = 2, \Lambda_1(t) = (t/10)^2$ ,  $n$  and  $N$  are shown for different curves in the figure, for the SARI $_{n,m}$  model.

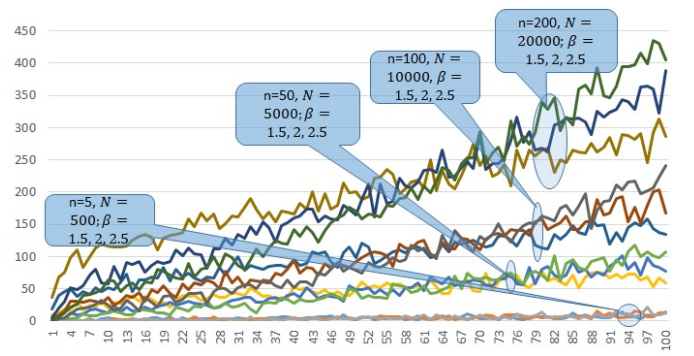


Figure 3:  $\rho_1 = 0.5, m = 2, \Lambda_1(t) = (t/10)^\beta$ ,  $n, N$  and  $\beta$  are shown in the figure message boxes, respectively, for the SARA $_{n,m}$  model.

#### 193 4. Modelling the failure process with masked failure data

194 If  $T_{k,N_k,t}$  (for  $k = 1, 2, \dots$ ) are known and we assume that  $\lambda_k(t) = \lambda(t)$  and  $\rho_k = \rho$ , from Eq. (7) and  
 195 Eq. (8), we obtain

$$\begin{aligned}
 \lambda_s(t) &= \frac{1}{n} \sum_{k=1}^n \left( \lambda_k(t) - \sum_{j=0}^{\min\{N_k,t-1, m_k-1\}} \rho_k (1 - \rho_k)^j \lambda_k(T_{k,N_k,t-j}) \right) \\
 &= \lambda(t) - \frac{1}{n} \sum_{j=0}^{\min\{N_k,t-1, m_k-1\}} \left( \rho(1 - \rho)^j \sum_{k=1}^n \lambda(T_{k,N_k,t-j}) \right), \tag{11}
 \end{aligned}$$

199 and

$$\begin{aligned}
\lambda_s(t) &= \frac{1}{n} \sum_{k=1}^n \lambda_k \left( t - \sum_{j=0}^{\min\{N_{k,t}-1, m_k-1\}} \rho_k (1 - \rho_k)^j T_{k, N_{k,t}-j} \right) \\
&= \frac{1}{n} \sum_{k=1}^n \lambda \left( t - \sum_{j=0}^{\min\{N_{k,t}-1, m_k-1\}} \rho (1 - \rho)^j T_{k, N_{k,t}-j} \right), \tag{12}
\end{aligned}$$

203 respectively.

204 Under the assumption that only masked failure data are available, unlike the SRP in which a component  
205 after a renewal can be regarded as starting from time 0, which implies the SRP model does not need to  
206 remember the component's previous maintenance/repair history. The  $\text{SARI}_{n,m}$  or the  $\text{SARA}_{n,m}$  processes,  
207 however, must remember all of its maintenance history. If we compare the SRP with the SIRP, we can find

- 208 • that the age of a component in the SRP is unknown as we do not know when it is installed;
- 209 • that the number of failures of a component in the SRP is always 1 as a failed component is renewed;
- 210 • that the operating/calendar age of a component in the SIRP is known as it is installed and started at  
211 time 0; and
- 212 • that the number of failures of a component in the SIRP is unknown.

213 In what follows, we assume the  $n$  components in the series system are identical. If the failure process  
214 of a component follows  $\text{ARI}_m$  (or  $\text{ARA}_m$ ), then the failure processes of the others should follow the same  
215 model.

216 Under the assumption that only masked failure data are available, the value  $k$ 's in  $T_{k, N_{k,t}}$  in Eq. (11) or  
217 in Eq. (4) are not observable. As such, it is not possible to use these two models shown in (11) and (4).

218 Under the assumption that only masked failure data are available, we may have two approaches to  
219 approximating the  $\text{SARI}_{n,m}$  process or the  $\text{SARA}_{n,m}$  process. These two approaches are

220 **Approach 1** to regard the system as one single item and approximate  $\text{SARI}_{n,m}$  and  $\text{SARA}_{n,m}$  with  $\text{ARI}_m$   
221 and  $\text{ARA}_m$ , respectively, or

222 **Approach 2** to take a further development of  $\text{SARI}_{n,m}$  and  $\text{SARA}_{n,m}$ , respectively, and propose new  
223 models to approximate these two models, respectively.

224 Approach 1 uses the  $\text{ARI}_m$  model and the  $\text{ARA}_m$  model to approximate the series system if the failure  
225 data are masked. That is, in this approach, one regards a multi-component system to be a one-component  
226 system, then use the  $\text{ARI}_m$  model or the  $\text{ARA}_m$  model to model the failure process.

227 When the number of failures is small, using the  $\text{ARI}_m$  or the  $\text{ARA}_m$  to approximate an SIRP makes the  
228 implicit assumption that the  $k$ th failure depends on the  $(k - 1)$ th, which may not be true for the case of

229  $N < n$  (where  $N$  is the total number of observed failures), under which each failed component may have  
 230 only experienced one failure, and the failures of different components are statistically independent. After  
 231 all, the probability of the occurrences of the first failures within a short time is greater than that of the  
 232 second failures because: within a given time period  $(0, t)$ , denote  $P(N(t) = k)$  as the probability that the  
 233 number of failures is  $k$ , then  $P(N(t) = 2) < P(N(t) = 1)$ .

234 Although the numbers of component failures in a typical system may be different, as shown in Fig 4,  
 235 the expected numbers of failures for identical components in a given time period are the same. As such, a  
 236 naive but appealing approach to approximating the SIRP model is to assume that the failures of the system  
 237 are caused by each component one after another. That is, suppose a system that is composed of identical  
 238 components in series, we assume the first  $n$  failures are due to the first failures of the  $n$  components, the  
 239 failures from the  $(n + 1)$ -th to the  $2n$ -th failures are due to the second failures of the  $n$  failures, and so on.  
 240 Based on this assumption, we have the following discussion.

241 Denote

$$242 \quad b_{N_t} = \begin{cases} N_t - n \lfloor \frac{N_t}{n} \rfloor & N_t \neq n \lfloor \frac{N_t}{n} \rfloor \\ n & N_t = n \lfloor \frac{N_t}{n} \rfloor, \end{cases} \quad (13)$$

243 where  $\lfloor x \rfloor$  is the largest integer that is smaller than or equal to  $x$ .

244 Then we have the following analyses.

245 (i) **The case of the ARI model.** If we assume that the failure process of each component follows  $\text{ARI}_m$   
 246 shown in Eq. (4), we have the following analyses.

- 247 • If  $N_t = 0$ , the failure intensity of the system is  $\lambda(t)$ .
- 248 • If  $0 < N_t \leq n$ , there are  $N_t$  components whose first failures occur. Each of these components has  
 249 failure intensity function  $\frac{1}{n}\lambda(t) - \frac{1}{n}\rho\lambda(T_k)$  and each of the rest  $n - N_t$  components has failure  
 250 intensity  $\frac{1}{n}\lambda(t)$ . As such, the failure intensity function of the system after the  $N_t$ -th failure is  
 251 given by

$$252 \quad \lambda_s^a(t) = \frac{1}{n} \sum_{k=1}^{N_t} (\lambda(t) - \rho\lambda(T_k)) + \frac{n - N_t}{n} \lambda(t)$$

$$253 \quad = \lambda(t) - \frac{1}{n} \sum_{k=1}^{N_t} \rho\lambda(T_k) \quad (14)$$

- 255 • If  $n < N_t \leq mn$ , there are the two following scenarios.
- 256 – If  $N_t = n \lfloor \frac{N_t}{n} \rfloor$ , then the failure intensity function of the system is given by

$$257 \quad \lambda_s^a(t) = \lambda(t) - \frac{1}{n} \sum_{k=1}^n \sum_{j=0}^{\lfloor \frac{N_t}{n} \rfloor - 1} \rho(1 - \rho)^j \lambda(T_{N_t - nj - k + 1}). \quad (15)$$

258 – If  $N_t \neq n \lfloor \frac{N_t}{n} \rfloor$ , then  $b_{N_t}$  components have experienced one more failure than the  $n - b_{N_t}$   
 259 other components. The sum of the failure intensity functions of these  $b_{N_t}$  components is  
 260  $\frac{b_{N_t}}{n} \lambda(t) - \frac{1}{n} \sum_{k=1}^{b_{N_t}} \sum_{j=0}^{\lfloor \frac{N_t}{n} \rfloor} \rho(1 - \rho)^j \lambda(T_{N_t - nj - k + 1})$ , and the sum of the failure intensity function of  
 261 the  $n - b_{N_t}$  other components is  $\frac{n - b_{N_t}}{n} \lambda(t) - \frac{1}{n} \sum_{k=b_{N_t} + 1}^n \sum_{j=0}^{\lfloor \frac{N_t}{n} \rfloor - 1} \rho(1 - \rho)^j \lambda(T_{N_t - nj - k + 1})$ . As  
 262 such, the failure intensity function of the system is given by

$$263 \lambda_s^a(t) = \lambda(t) - \frac{1}{n} \sum_{k=1}^{b_{N_t}} \sum_{j=0}^{\lfloor \frac{N_t}{n} \rfloor} \rho(1 - \rho)^j \lambda(T_{N_t - nj - k + 1}) - \frac{1}{n} \sum_{k=b_{N_t} + 1}^n \sum_{j=0}^{\lfloor \frac{N_t}{n} \rfloor - 1} \rho(1 - \rho)^j \lambda(T_{N_t - nj - k + 1}).$$

264 (16)

265 • Similar to the case of  $n < N_t \leq mn$ , if  $N_t > mn$ , then we have

266 – If  $N_t = n \lfloor \frac{N_t}{n} \rfloor$ , then the failure intensity function of the system is given by

$$267 \lambda_s^a(t) = \lambda(t) - \frac{1}{n} \sum_{k=1}^n \sum_{j=0}^{m-1} \rho(1 - \rho)^j \lambda(T_{N_t - nj - k + 1}),$$

268 (17)

268 – If  $N_t \neq n \lfloor \frac{N_t}{n} \rfloor$ , the failure intensity function of the system is given by

$$269 \lambda_s^a(t) = \lambda(t) - \frac{1}{n} \sum_{k=1}^{b_{N_t}} \sum_{j=0}^{m-1} \rho(1 - \rho)^j \lambda(T_{N_t - nj - k + 1}) - \frac{1}{n} \sum_{k=b_{N_t} + 1}^n \sum_{j=0}^{m-1} \rho(1 - \rho)^j \lambda(T_{N_t - nj - k + 1})$$

270 (18)

271 (ii) **The case of the ARA model.** If we assume that the failure process of each component follows  
 272 ARA<sub>m</sub> shown in Eq. (5), we have the following analyses.

- 273 • If  $N_t = 0$ , the failure intensity of the system is  $\lambda(t)$ .
- 274 • If  $0 < N_t \leq n$ , there are  $N_t$  components whose first failures occur. Each of these components has  
 275 failure intensity function  $\frac{1}{n} \lambda(t - \rho T_k)$  and each of the rest  $n - N_t$  components has failure intensity  
 276  $\frac{1}{n} \lambda(t)$ . As such, the failure intensity function of the system after the  $N_t$ -th failure is given by

$$277 \lambda_s^a(t) = \frac{1}{n} \sum_{k=1}^{N_t} \lambda(t - \rho T_k) + \frac{n - N_t}{n} \lambda(t)$$

278 (19)

- 279 • If  $N_t > n$ , a similar discussion as the ARI case can be made.

280 To sum up, we obtain the following definition, i.e., Definition 1.

281 **Definition 1.** A new SARI<sub>n,m</sub> model, denoted as SARI<sub>n,m</sub><sup>a</sup>, and a new SARA<sub>n,m</sub>, denoted as SARA<sub>n,m</sub><sup>a</sup> are  
 282 defined, respectively, in the following. A SARI<sub>n,m</sub><sup>a</sup> is defined by

$$283 \quad \lambda_s^a(t) = \begin{cases} \lambda(t), & \text{if } N_t < 1; \\ \lambda(t) - \frac{1}{n} \sum_{k=1}^{N_t} \rho \lambda(T_k), & \text{if } 1 \leq N_t < n; \\ \lambda(t) - \frac{1}{n} \sum_{k=1}^{b_{N_t}} \rho \lambda(T_{N_t-k+1}) - \frac{1}{n} \sum_{k=1}^n \sum_{j=1}^{\min\{\lfloor \frac{N_t}{n} \rfloor - 1, m-1\}} \rho(1-\rho)^j \lambda(T_{N_t-n(j-1)-b_{N_t}-k+1}) & \text{if } N_t \geq n \end{cases} \quad (20)$$

284 and a SARA<sub>n,m</sub><sup>a</sup> is defined by

$$285 \quad \lambda_s^a(t) = \begin{cases} \lambda(t), & \text{if } N_t < 1; \\ \frac{1}{n} \sum_{k=1}^{N_t} \lambda(t - \rho T_k) + \frac{n - N_t}{n} \lambda(t), & \text{if } 1 \leq N_t < n; \\ \frac{1}{n} \sum_{k=1}^{b_{N_t}} \lambda(t - \rho T_{N_t-k+1}) + \frac{1}{n} \sum_{k=1}^n \lambda \left( t - \sum_{j=1}^{\min\{\lfloor \frac{N_t}{n} \rfloor - 1, m-1\}} \rho(1-\rho)^j T_{N_t-n(j-1)-b_{N_t}-k+1} \right) & \text{if } N_t \geq n \end{cases} \quad (21)$$

286

287 On Definition 1, there are the following special cases.

288 (i) If  $n = 1$ , then SARI<sub>n,m</sub><sup>a</sup> in Eq. (20) and SARA<sub>n,m</sub><sup>a</sup> in Eq. (21) reduce to ARI<sub>m</sub> and ARA<sub>m</sub> in (4) and  
 289 (5), respectively.

290 (ii) If  $m = 1$  and  $N_t > n$ , then SARI<sub>n,m</sub><sup>a</sup> reduces to SARI<sub>n,1</sub>,

$$291 \quad \lambda_s^a(t) = \lambda(t) - \frac{1}{n} \sum_{k=1}^n \rho \lambda(T_{N_t-k+1}), \quad (22)$$

292 and, SARA<sub>n,m</sub><sup>a</sup> reduces to SARA<sub>n,1</sub>,

$$293 \quad \lambda_s^a(t) = \frac{1}{n} \sum_{k=1}^n \lambda(t - \rho T_{N_t-k+1}). \quad (23)$$

294 (iii) If  $\rho = 0$ , then the repair on each component is minimal and both SARI<sub>n,m</sub><sup>a</sup> in Eq. (20) and SARA<sub>n,m</sub><sup>a</sup>  
 295 in Eq. (21) reduce the NHPP (non-homogenous Poisson process).

296 (iv) If  $\rho = 1$  and  $n = 1$ , then

- 297 • The failure intensity  $\lambda_s^a(t)$  after the  $N_t$ th failure in SARI<sub>1,m</sub> (see Eq. (20)) is  $\lambda(t) - \lambda(T_{N_t})$ . At  
 298 time  $T_{N_t}$ ,  $\lambda(t) - \lambda(T_{N_t}) = 0$  and the system starts from the status with failure intensity 0. But  
 299 it is important to note that it does not mean that the item is repaired as good as new.
- 300 • The failure intensity  $\lambda_s^a(t)$  after the  $N_t$ th failure in the SARA<sub>1,m</sub> model (see Eq. (21)) is  $\lambda(t - T_{N_t})$ .  
 301 At time  $T_{N_t}$ ,  $\lambda(t - T_{N_t}) = 0$ , which implies that the system is repaired as good as new.

302 (v) If  $\rho = 1$  and  $n > 1$ , model Eq. (20) and model Eq. (21) reduce to

$$303 \quad \lambda_s^a(t) = \lambda(t) - \frac{1}{n} \sum_{k=1}^n \lambda(T_{N_t-k+1}), \quad (24)$$

304 and

$$305 \quad \lambda_s^a(t) = \frac{1}{n} \sum_{k=1}^n \lambda(t - T_{N_t-k+1}), \quad (25)$$

306 respectively.

307 The model shown in Eq. (25) is the MAI model, which is a special case of the model shown in Eq.  
308 (3).

309 **Remark 1.** *The above bullet (v) shows that the MAI model is a special case of the  $SARA_{n,m}^a$  model.*  
310 *Numerical data experiments and case studies show that the MAI model has a clear advantage over ten other*  
311 *models on 11 out of 15 real world datasets [4]. As such, the model  $SARA_{n,m}^a$  can be regarded as an extension*  
312 *of the MAI model.*

313 **Remark 2.** *The existing failure process models can roughly be categorised into three classes, as discussed*  
314 *below.*

- 315 • *Models that have one parameter depicting the repair effectiveness of each individual repair. For exam-*  
316 *ple, the parameter  $A_n$  in the virtual age models  $V_n = V_{n-1} + A_n(T_n - T_{n-1})$  and  $V_n = A_n(V_{n-1} + T_n -$   
317  $T_{n-1})$  is the parameter depicting the effectiveness of the  $n$ th repair [25] (where  $V_n$  is the virtual age).*  
318 *Technically,  $A_n$  may estimate the repair effectiveness of different components in a system. However,*  
319 *in reality, it is not suitable for modelling the failure process of a multi-component system due to two*  
320 *reasons: on the one hand, the size of masked failure data may not be sufficiently large for estimating a*  
321 *large number of parameters  $A_n$ ; on the other hand,  $A_n$  may be assumed a stochastic process, on which*  
322 *there is little research that has been conducted.*
- 323 • *Models that have only one parameter depicting the repair effectiveness for different components in*  
324 *a system. For example, models shown in Eq. (4) and (5) fall in this category. Similarly, if  $A_n$*   
325 *in the virtual age models are set to  $A_n = A$  (i.e.,  $A_n$  are the same over different  $n$ 's), then the*  
326 *above-mentioned virtual age models have one parameter as well. The shortcoming of such models for*  
327 *modelling the failure process of a multi-component system is discussed in Approach 1 in the above*  
328 *discussion.*
- 329 • *Models that approximates the SRP. For example, models shown in Eqs. (1), (2) and (3) fall in this*  
330 *category, which assumes that the repair on each failed component is perfect and is not suitable for a*  
331 *system in which repair on failed component is imperfect.*

332 Models (20) and (21) are derived for depicting the failure process of a multi-component series system when  
 333 the failure process of a component follows the ARI model and the ARA model, respectively. They can  
 334 therefore be used to model the failure process of the pavement system discussed in Section 1, for example.

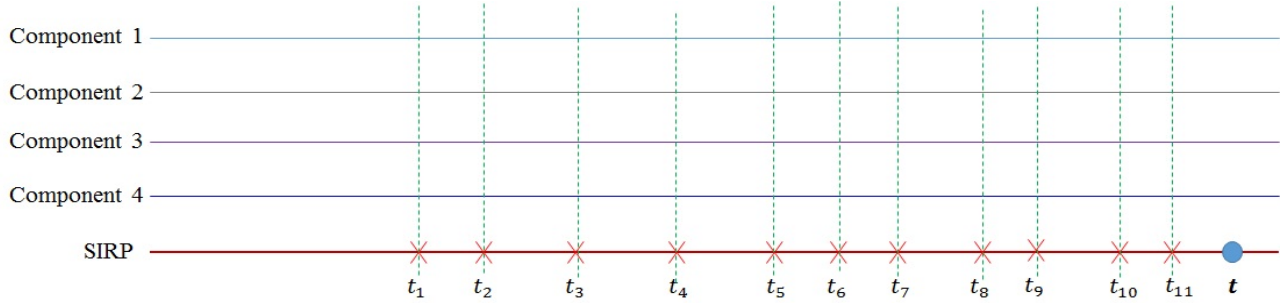


Figure 4: Masked failure data of a system with four components until time  $t$ , where  $N_{1,t}, N_{2,t}, N_{3,t}$ , and  $N_{4,t}$  are unknown;  $N_t = 11$ . where  $t_{i,0} = 0$ ,  $j = 1, 2, \dots, N_{i,t}$ , and  $t_j = 0$  if  $j \leq 0$ .

335 **Example 2.** Suppose that the value  $k$ 's in  $T_{k,j}$  in Example 1 are unknown. But  $t_j$  ( $j = 1, 2, \dots, 11$ ) are  
 336 available, as shown in Figure 4. We assume that the four components are identical and that the failure  
 337 process of each component is  $ARI_3$ . The 11 failures are assumed to be caused by three failures of each of  
 338 three components and two failures of the other component ( $3 \times 3 + 2 = 11$ ), respectively, which can be modelled  
 339 by Model (20) in Definition 1. The model,  $SARI_{4,3}^a$ , is given by

$$\begin{aligned}
 340 \quad \lambda_s^a(t) &= \lambda(t) - \frac{1}{4}\rho(\lambda(t_{11}) + \lambda(t_{10}) + \lambda(t_9)) \\
 341 &\quad - \frac{1}{4}\rho(1 - \rho)(\lambda(t_8) + \lambda(t_7) + \lambda(t_6) + \lambda(t_5)) \\
 342 &\quad - \frac{1}{4}\rho(1 - \rho)^2(\lambda(t_4) + \lambda(t_3) + \lambda(t_2) + \lambda(t_1)). \tag{26} \\
 343
 \end{aligned}$$

344 In case the causes of the system failures are known, then by plugging  $t_{k,i}$  in Figure 3 into Eq. (26), we obtain

$$\begin{aligned}
 345 \quad \lambda_s^a(t) &= \lambda(t) - \frac{1}{4}\rho(\lambda(t_{1,3}) + \lambda(t_{4,5}) + \lambda(t_{4,4})) \\
 346 &\quad - \frac{1}{4}\rho(1 - \rho)(\lambda(t_{2,2}) + \lambda(t_{4,3}) + \lambda(t_{4,2}) + \lambda(t_{1,2})) \\
 347 &\quad - \frac{1}{4}\rho(1 - \rho)^2(\lambda(t_{3,1}) + \lambda(t_{2,1}) + \lambda(t_{4,1}) + \lambda(t_{1,1})). \tag{27} \\
 348
 \end{aligned}$$

349 As can be seen, Model (27) differs from Model (6).

350 In the following, we compare  $\lambda_s(t)$  in Eq. (7) with  $\lambda_s^a(t)$  in Eq. (20), and  $\lambda_s(t)$  in (8) with  $\lambda_s^a(t)$  in (21).  
 351 To do it, we need to introduce an important definition on stochastic ordering.

352 **Definition 2.** Stochastic order (p. 404 in [26]). Assume that  $X$  and  $Y$  are two random variables. If for  
 353 every real number  $r$ , the inequality

$$P(X \geq r) \geq P(Y \geq r)$$

355 holds, then  $X$  is stochastically greater than or equal to  $Y$ , or  $X \geq_{st} Y$ . Equivalently,  $Y$  is stochastically less  
 356 than or equal to  $X$ , or  $Y \leq_{st} X$ , or,  $E(X) \geq E(Y)$ .

357 Suppose a system is composed of  $n$  identical components, each of which follows the same  $\text{ARI}_m$ , then  
 358 for  $N_t > n$  we have

$$\begin{aligned}
 359 \quad \lambda_s(t) &= \lambda(t) - \frac{1}{n} \sum_{k=1}^n \sum_{j=0}^{\min\{m-1, N_{k,t}-1\}} \rho(1-\rho)^j \lambda(T_{k, N_{k,t}-j}) \\
 360 \quad &= \lambda(t) - \frac{1}{n} \sum_{k=1}^{b_{N_t}} \rho \lambda(T_{N_t-k+1}) - \frac{1}{n} \sum_{k=1}^n \sum_{j=1}^{\min\{\lfloor \frac{N_t}{n} \rfloor - 1, m-1\}} \rho(1-\rho)^j \lambda(T_{N_t-n(j-1)-b_{N_t}-k+1}) + \epsilon_t, \quad (28) \\
 361
 \end{aligned}$$

362 where

$$\begin{aligned}
 363 \quad \epsilon_t &= -\frac{1}{n} \sum_{k=1}^n \sum_{j=0}^{\min\{m-1, N_{k,t}-1\}} \rho(1-\rho)^j \lambda(T_{k, N_{k,t}-j}) \\
 364 \quad &+ \frac{1}{n} \sum_{k=1}^{b_{N_t}} \rho \lambda(T_{N_t-k+1}) + \frac{1}{n} \sum_{k=1}^n \sum_{j=1}^{\min\{\lfloor \frac{N_t}{n} \rfloor - 1, m-1\}} \rho(1-\rho)^j \lambda(T_{N_t-n(j-1)-b_{N_t}-k+1}). \\
 365
 \end{aligned}$$

366 **Lemma 2.** *The expectation of  $\epsilon_t$  has the following bounds:*

$$367 \quad -\frac{1-\rho^m}{1-\rho} E(\lambda(T_1)) \leq E(\epsilon_t) \leq \rho E(\lambda(T_1)) + \frac{1-\rho^m}{1-\rho} E(\lambda(T_1)) \quad (29) \\
 368$$

369 The proof of Lemma 2 can be found in Appendix.

370  $\epsilon_t$  measures the difference between  $\lambda_s(t)$  and  $\lambda_s^a(t)$ . It should be noted:  $\epsilon_t$  has a practical implication if  
 371 the values of  $\rho$ 's in Eq. (11) and in Eq. (20) are the same and the  $\lambda(t)$  in model (20), which is obtained  
 372 from the masked failure data, and the  $\lambda(t)$  in model (11), which is obtained from the unmasked failure data  
 373 are the same.

## 374 5. Parameter estimation and numerical examples

375 In this section, we derive the maximum likelihood functions for the models proposed in Section 4 and  
 376 then apply them on a real dataset.

377 Given a series of successive failure times  $t_1, t_2, \dots, t_N$ , on which the system failed; where  $N$  is the number  
 378 of failures and  $N > n$ . That is, the available data are up to the time at which the last failure occurs.

### 379 5.1. Maximum likelihood functions

380 Below we consider the likelihood for the failure process of a single system before a specified number of  
 381 failures is occurred. If several independent processes are observed, the log-likelihood can be easily obtained  
 382 based on the likelihood functions given in this section.

383 Below we will give the likelihood function of the  $\text{SARI}_{n,m}^a$  model and the  $\text{SARA}_{n,m}$  models in Section  
 384 3. The derivation of the likelihood functions follows from Andersen et al. (1993, sec. II.7) that under our  
 385 stated conditions, the likelihood function for the observations from a single system is derived below.

386 Following the definition of  $b_{N_i}$ , we define  $b_i = i - n \lfloor \frac{i}{n} \rfloor$  if  $i \neq n \lfloor \frac{i}{n} \rfloor$ , where  $i$  is a positive integer. We also  
 387 define  $\mathbb{N}_1 = \{i | 1 \leq i \leq n-1\}$ ,  $\mathbb{N}_2 = \{i | n < i \leq N-1, i \neq \nu n, 1 \leq \nu < \lfloor \frac{N}{n} \rfloor\}$ , and  $\mathbb{N}_3 = \{i | i = \nu n, \nu < \lfloor \frac{N}{n} \rfloor\}$ .

388 Hence, given a dataset of  $N$  successive failure times  $t_1, \dots, t_N$ , the likelihood function for the  $\text{SARI}_{n,m}^a$   
 389 model is

$$\begin{aligned}
 390 \quad L_{\text{SARI}}(\Theta) &= \lambda(t_1) \exp(-\Lambda(t_1)) \prod_{i \in \mathbb{N}_1} \left[ \left( \lambda(t_{i+1}) - \frac{1}{n} \sum_{k=1}^i \rho \lambda(t_k) \right) \exp \left( -\Lambda(t_{i+1}) + \Lambda(t_i) + \frac{(t_{i+1} - t_i)}{n} \sum_{k=1}^i \rho \lambda(t_k) \right) \right] \\
 391 \quad &\times \prod_{i \in \mathbb{N}_2} \left[ \left( \lambda(t_{i+1}) - \frac{1}{n} \sum_{k=1}^{b_i} \sum_{j=0}^{\min\{\lfloor \frac{i}{n} \rfloor, m-1\}} \rho(1-\rho)^j \lambda(t_{i-nj-k+1}) - \frac{1}{n} \sum_{k=b_i+1}^n \sum_{j=0}^{\min\{\lfloor \frac{i}{n} \rfloor - 1, m-1\}} \rho(1-\rho)^j \lambda(t_{i-nj-k+1}) \right) \right. \\
 392 \quad &\times \exp \left( -\Lambda(t_{i+1}) + \frac{(t_{i+1} - t_i)}{n} \sum_{k=1}^{b_i} \sum_{j=0}^{\min\{\lfloor \frac{i}{n} \rfloor, m-1\}} \rho(1-\rho)^j \lambda(t_{i-nj-k+1}) \right. \\
 393 \quad &\left. \left. + \Lambda(t_i) + \frac{(t_{i+1} - t_i)}{n} \sum_{k=b_i+1}^n \sum_{j=0}^{\min\{\lfloor \frac{i}{n} \rfloor - 1, m-1\}} \rho(1-\rho)^j \lambda(t_{i-nj-k+1}) \right) \right] \\
 394 \quad &\times \prod_{i \in \mathbb{N}_3} \left[ \left( \lambda(t_{i+1}) - \frac{1}{n} \sum_{k=1}^n \sum_{j=0}^{\min\{\lfloor \frac{i}{n} \rfloor - 1, m-1\}} \rho(1-\rho)^j \lambda(t_{i-nj-k+1}) \right) \right. \\
 395 \quad &\left. \times \exp \left( -\Lambda(t_{i+1}) + \Lambda(t_i) + \frac{(t_{i+1} - t_i)}{n} \sum_{k=1}^n \sum_{j=0}^{\min\{\lfloor \frac{i}{n} \rfloor - 1, m-1\}} \rho(1-\rho)^j \lambda(t_{i-nj-k+1}) \right) \right] \quad (30)
 \end{aligned}$$

397 and the likelihood of the  $\text{SARA}_{n,m}^a$  model is given by

$$\begin{aligned}
 398 \quad L_{\text{SARA}}(\Theta) &= \lambda(t_1) \exp(-\Lambda(t_1)) \\
 399 \quad &\times \prod_{i \in \mathbb{N}_1} \left\{ \left[ \frac{n-i}{n} \lambda(t_{i+1}) + \frac{1}{n} \sum_{k=1}^i \lambda(t_{i+1} - \rho t_k) \right] \exp \left( -\frac{1}{n} \sum_{k=1}^i \Lambda(t_{i+1} - \rho t_k) + \frac{1}{n} \sum_{k=1}^i \Lambda(t_i - \rho t_k) - \frac{n-i}{n} (\Lambda(t_{i+1}) - \Lambda(t_i)) \right) \right\} \\
 400 \quad &\times \prod_{i \in \mathbb{N}_2} \left\{ \left[ \frac{1}{n} \sum_{k=1}^{b_i} \lambda \left( t_{i+1} - \sum_{j=0}^{\min\{\lfloor \frac{i}{n} \rfloor, m-1\}} \rho(1-\rho)^j t_{i-nj-k+1} \right) + \frac{1}{n} \sum_{k=b_i+1}^n \lambda \left( t_{i+1} - \sum_{j=0}^{\min\{\lfloor \frac{i}{n} \rfloor - 1, m-1\}} \rho(1-\rho)^j t_{i-nj-k+1} \right) \right] \right. \\
 401 \quad &\times \exp \left[ -\frac{1}{n} \sum_{k=1}^{b_i} \Lambda \left( t_{i+1} - \sum_{j=0}^{\min\{\lfloor \frac{i}{n} \rfloor, m-1\}} \rho(1-\rho)^j t_{i-nj-k+1} \right) - \frac{1}{n} \sum_{k=b_i+1}^n \Lambda \left( t_{i+1} - \sum_{j=0}^{\min\{\lfloor \frac{i}{n} \rfloor - 1, m-1\}} \rho(1-\rho)^j t_{i-nj-k+1} \right) \right. \\
 402 \quad &\left. \left. + \frac{1}{n} \sum_{k=1}^{b_i} \Lambda \left( t_i - \sum_{j=0}^{\min\{\lfloor \frac{i}{n} \rfloor, m-1\}} \rho(1-\rho)^j t_{i-nj-k+1} \right) + \frac{1}{n} \sum_{k=b_i+1}^n \Lambda \left( t_i - \sum_{j=0}^{\min\{\lfloor \frac{i}{n} \rfloor - 1, m-1\}} \rho(1-\rho)^j t_{i-nj-k+1} \right) \right] \right\} \\
 403 \quad &\times \prod_{i \in \mathbb{N}_3} \left\{ \frac{1}{n} \sum_{k=1}^n \lambda \left( t_{i+1} - \sum_{j=0}^{\min\{\lfloor \frac{i}{n} \rfloor - 1, m-1\}} \rho(1-\rho)^j t_{i-nj-k+1} \right) \right. \\
 404 \quad &\left. \times \exp \left[ -\frac{1}{n} \sum_{k=1}^n \Lambda \left( t_{i+1} - \sum_{j=0}^{\min\{\lfloor \frac{i}{n} \rfloor - 1, m-1\}} \rho(1-\rho)^j t_{i-nj-k+1} \right) + \frac{1}{n} \sum_{k=1}^n \Lambda \left( t_i - \sum_{j=0}^{\min\{\lfloor \frac{i}{n} \rfloor - 1, m-1\}} \rho(1-\rho)^j t_{i-nj-k+1} \right) \right] \right\}, \quad (31)
 \end{aligned}$$

406 where  $t_0 = 0$ ,  $\lambda(t) = 0$ , and  $\Lambda(t) = \int_0^t \lambda(u) du$ .

407 By maximising  $\log(L_{\text{SARI}})$  and  $\log(L_{\text{SARA}})$ , one can find optimal parameters in  $\lambda(t)$  and  $\hat{\rho}$ , respectively.

408 5.2. Data examples

409 In the following, we compare the performance of models NHPP,  $ARI_m$ ,  $ARA_m$ ,  $SARI_{n,m}^a$ , and  $SARA_{n,m}^a$ .  
 410 We use criteria such AIC (Akaike information criterion),  $AIC_c$  (AIC with a correction), and BIC (Bayesian  
 411 information criterion) to compare the performance. Those criteria are:  $AIC = -2\log(L) + 2q$ ,  $AIC_c =$   
 412  $-2\log(L) + 2q + \frac{2(q+2)(q+3)}{N-q-2}$ , and  $BIC = -2\log(L) + q\log(N)$ , where  $L$  is the maximized value of  
 413 the likelihood for the model,  $q$  is the number of parameters in the model, and  $N$  is the total number of  
 414 failures (observations). The term  $2q$ ,  $\frac{2(q+2)(q+3)}{N-q-2}$ , and  $q\log(N)$  in the AIC,  $AIC_c$  and BIC penalise a  
 415 model with a large number of parameters, respectively. The reader is referred to [27] for details on model  
 416 performance measures. [28] provides a practical procedure for the selection of time-to-failure models based  
 417 on the assessment of trends in maintenance data.

418 We compare the performance of the proposed models  $SARI_{n,m}^a$  and  $SARA_{n,m}^a$  on artificially generated  
 419 data, which are generated based on the simulation method shown in Section 3.3. We set failure intensity  
 420 function  $\lambda(t) = 0.002869t^{1.5}$  (which has  $\Lambda(t) = (\frac{t}{15})^{2.5}$ ),  $n = 3$ ,  $m = 2$ , and  $\rho = 0.5$ , that is, each of the three  
 421 components has a failure process  $ARI_2$ . We compare the models: NHPP, ESI, MAI, ARI, ARA,  $SARI_{n,m}^a$ ,  
 422 and  $SARA_{n,m}^a$  on the dataset. Table 2 shows that the  $SARI_{3,7}$  outperforms other models in terms of the  
 423  $-\log(\text{likelihood})$ .

Table 2: Model comparison on artificially generated data.

		NHPP	ESI	MAI	ARI	ARA	SARI	SARA
SARI Data	$-\log(\text{likelihood})$	85.78	85.14	85.13	84.10	84.14	84.09	84.12
$(\alpha = 15, \beta = 2.5$ $n = 3, N = 50)$	BIC	179.38	182.01	178.09	179.94	180.01	179.92	179.97
	$AIC_c$	176.08	177.16	174.79	175.09	175.16	175.07	175.12

424 We also compare the performance of the proposed models  $SARI_{n,m}^a$  and  $SARA_{n,m}^a$  on the Bus514 dataset  
 425 shown in [29]. On this dataset, we know neither the number of components nor whether the components are  
 426 identical. We compare the models: NHPP, ESI, MAI, ARI, ARA,  $SARI_{n,m}^a$ , and  $SARA_{n,m}^a$  on the dataset.  
 Table 3 shows that the  $SARI_{3,1}^a$  outperforms other models.

Table 3: Model comparison on the Bus514 dataset.

		NHPP	ESI	MAI	ARI	ARA	SARI	SARA
Bus514 Data	$-\log(\text{likelihood})$	532.74	530.82	533.18	530.84	532.74	<u>530.38</u>	532.74
	BIC	1073.46	1073.61	1074.34	1073.65	1077.45	<u>1072.73</u>	1077.45
	$AIC_c$	1069.96	1068.46	1070.84	1068.50	1072.30	<u>1067.58</u>	1072.30

427  
 428 The above two examples show that  $SARI_{n,m}^a$  results in the smallest  $-\log(\text{likelihood values})$ , but  $SARA_{n,m}^a$   
 429 does not perform so well as the  $SARI_{n,m}^a$  model. Nevertheless, since the MAI model shows its outstanding

430 performance and  $SARA_{n,m}^a$  is an extension of MAI, one may set  $\rho = 1$  in  $SARI_{n,m}^a$  in case  $SARA_{n,m}^a$  shows  
 431 poor performance on a dataset. To gain a better view on the comparison of the performance of the models,  
 Figure 5 shows their values of BIC and  $AIC_c$ .

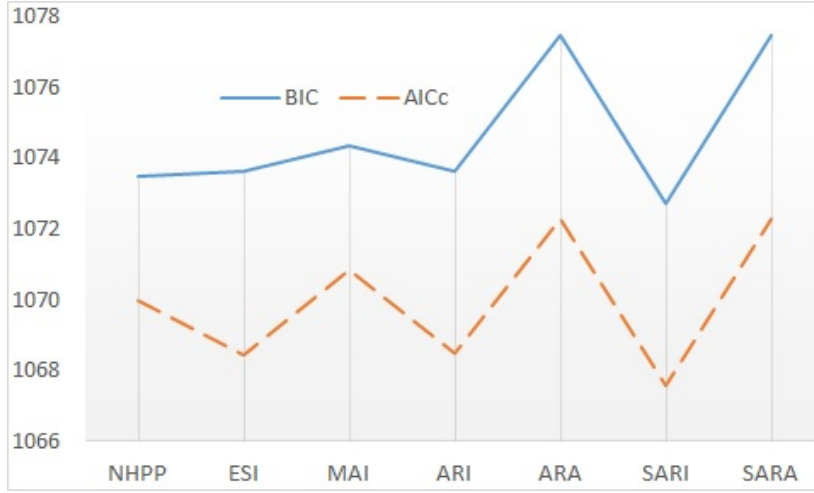


Figure 5: Comparison of BIC and  $AIC_c$ .

432

## 433 6. Discussion

### 434 6.1. An approximation method for left-truncated masked failure data

435 Section 4 discusses the scenario where a full history of masked failure data can be collected. Now we  
 436 consider the case that  $M$  failure observations of the earliest occurrences are not available, that is,  $T_1, \dots, T_M$   
 437 are not available, but  $T_{M+1}, T_{M+2}, \dots, T_{N_t}$  are available. Such data are *masked left-truncated failure data*.  
 438 One can use the models  $SARI_{n,m}^a$  and  $SARA_{n,m}^a$  in Section 4 to fit the data, which assumes that the first  $n$  failures  
 439 are due to the  $n$  components, respectively. An alternative method is to simply take  $T_{N_t}, T_{N_t-1}, \dots, T_{N_t-n+1}$   
 440 as the last failure times of the  $n$  components, and take  $T_{N_t-n}, T_{N_t-1}, \dots, T_{N_t-2n+1}$  as the 2nd last failure  
 441 times of the  $n$  components, and so on. Under such an assumption, we propose the following models.

442 **Definition 3.** A  $SARI_{n,m}^a$  is defined by

$$443 \lambda_s^a(t) = \lambda(t) - \frac{\Phi_{N_t'}}{n} \sum_{k=1}^n \sum_{j=0}^{\min\{\lfloor \frac{N_t'}{n} \rfloor - 1, m-1\}} \rho(1-\rho)^j \lambda(T_{N_t' - nj - k + 1}) - \frac{\Psi_{N_t'}}{n} \sum_{k=1}^{r_t} \rho(1-\rho)^{\lfloor \frac{N_t'}{n} \rfloor} \lambda(T_{N_t' - n \lfloor \frac{N_t'}{n} \rfloor - k + 1}), \quad (32)$$

444 and a  $SARA_{n,m}^a$  is defined by

$$445 \lambda_s^a(t) = \frac{\Phi_{N_t'}}{n} \sum_{k=1}^n \lambda \left( t - \sum_{j=0}^{\min\{\lfloor \frac{N_t'}{n} \rfloor - 1, m-1\}} \rho(1-\rho)^j T_{N_t' - nj - k + 1} \right) + \frac{\Psi_{N_t'}}{n} \sum_{k=1}^n \lambda \left( t - \sum_{k=1}^{r_t} \rho(1-\rho)^{\lfloor \frac{N_t'}{n} \rfloor} T_{N_t' - n \lfloor \frac{N_t'}{n} \rfloor - k + 1} \right), \quad (33)$$

446 where  $m \geq 1$ ,  $N'_t = N_t - M + 1$ ,  $\Phi_{N'_t} = \chi\{N'_t \geq n\}$ ,  $\Psi_{N'_t} = \chi\{\lfloor \frac{N'_t}{n} \rfloor < m \cap b_{N'_t} \neq 0\}$ ,  $r_t = N'_t - n\lfloor \frac{N'_t}{n} \rfloor$  if  
 447  $N'_t \neq n\lfloor \frac{N'_t}{n} \rfloor$ , and  $r_t = N'_t$  otherwise.

448 Definition 3 differs from Definition 1, as shown in Figure 6 and Example 3

- 449 • Fig. 6 shows the difference between the two definitions. The notes above the SIRP line shows how Definition  
 450 1 defines a cycle, which is a set of  $T_k$  with the same power of  $(1 - \rho)$  in a  $SARI_{n,m}^a$  model or in a  $SARA_{n,m}^a$   
 451 model, and the notes under the SIRP line shows how Definition 3 defines a cycle.
- 452 • Eq. (34) in Example 3 shows the  $SARI_{4,3}^a$  by Definition 3, in which  $\lambda(t_8)$  has a coefficient  $\frac{1}{4}\rho$  and  $\lambda(t_5)$  has a  
 453 coefficient  $\frac{1}{4}\rho(1 - \rho)$  whereas in Example 2,  $\lambda(t_8)$  has a coefficient  $\frac{1}{4}\rho(1 - \rho)$  and  $\lambda(t_5)$  has a coefficient  $\frac{1}{4}\rho$ .

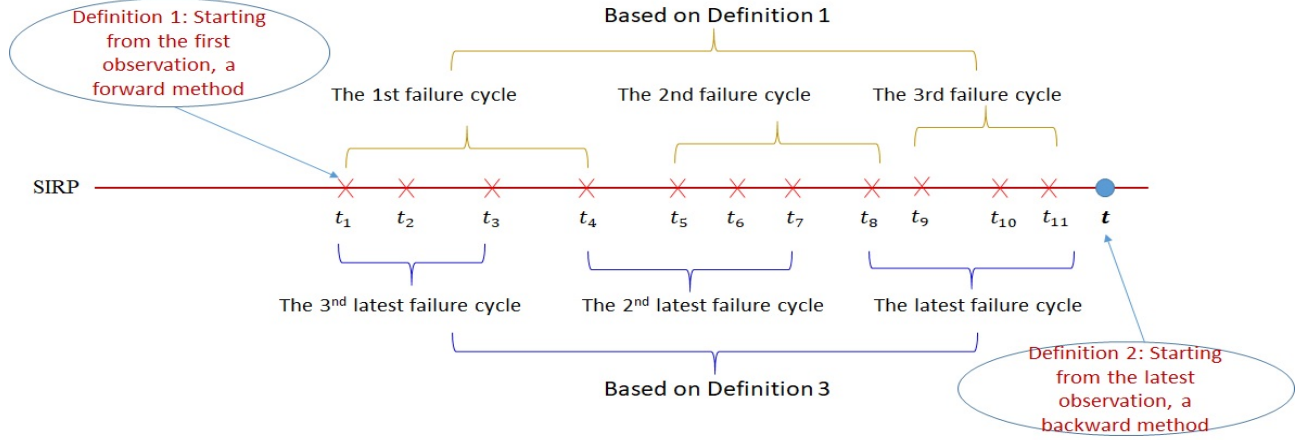


Figure 6: Comparison of definitions of different cycles of Definition 1 and Definition 2.

**Example 3.** Further to Example 2, a model  $SARI_{4,3}^a$ , defined by Definition 3, and is given by

$$\begin{aligned}
 \lambda_s^a(t) = & \lambda(t) - \frac{1}{4}\rho(\lambda(t_{11}) + \lambda(t_{10}) + \lambda(t_9) + \lambda(t_8)) \\
 & - \frac{1}{4}\rho(1 - \rho)(\lambda(t_7) + \lambda(t_6) + \lambda(t_5) + \lambda(t_4)) \\
 & - \frac{1}{4}\rho(1 - \rho)^2(\lambda(t_3) + \lambda(t_2) + \lambda(t_1)).
 \end{aligned} \tag{34}$$

## 454 6.2. Failure intensity function of the SRP

455 Although the SRP has been well studied (see [3] for more detailed discussion), to the author's best knowledge, its  
 456 failure intensity function has not been given in the existing literature and is given in Lemma 3.

457 **Lemma 3.** Given a series system on which a failed component is replaced with an identical new component immedi-  
 458 ately, the failure intensity function of the system after the  $N_t$ -th replacement is given by

$$\lambda(t|\mathcal{H}_{t-}) = \begin{cases} \frac{1}{n} \sum_{k=1}^n \lambda_k(t), & \text{if } N_t = 0, \\ \frac{1}{n} \sum_{k=1}^{n-1} \lambda_{i_k}(t - T_{i_k, N_t - j_k}) + \frac{1}{n} \lambda_{i_n}(t - T_{i_n, N_t}), & \text{if } N_t \geq 1. \end{cases} \tag{35}$$

460 where  $j_k \in \{1, 2, \dots, N_t\}$ ,  $i_k \in \{1, 2, \dots, n\}$ ,  $T_0 = 0$ ,  $i_{k_1} \neq i_{k_2}$  for  $k_1 \neq k_2$ ,  $j_{k_1} \neq j_{k_2}$  if  $k_1 \neq k_2$  and  $j_{k_1} j_{k_2} > 0$ .

461 The proof of Lemma 3 can be found in Appendix.

## 462 7. Conclusions and further work

463 In the real world, systems are normally composed of multiple components and the failure data may be masked  
464 due to insufficient failure cause data or such data are unattainable because of physical constraints or lack of resources.  
465 This needs to develop a method to model the superposition of a number of imperfect failure processes. However,  
466 since the failure data are masked, the components that cause the system to fail are unknown. This needs to develop  
467 methods to approximate the failure process of the system.

468 While the superposition of renewal processes has been extensively studied, the superposition of imperfect failure  
469 processes (SIRP) has received little attention in the literature. There is a need to conduct research on SIRP, which is  
470 the focus of this paper.

471 The main contributions of this paper include the following.

- 472 • This paper developed two methods: one for untruncated masked failure data and one for left-truncated data, to  
473 approximate the superposition of the imperfect failure processes of the components in a series system in which  
474 the failure process of each component follows two widely used models. The imperfect failure process models are  
475 the arithmetic reduction of intensity (ARI) model or the arithmetic reduction of age (ARA) model, respectively.
- 476 • The paper showed that unlike the superposition of renewal processes, the superposition of the ARI processes  
477 (SARI) (or the ARA processes (SARA)) does not tend toward (statistical) equilibrium as the time of operation  
478 becomes very large;
- 479 • The MAI (Moving Average of Intensity) model proposed in [4] is a special case of the superposition of the ARA  
480 processes; and
- 481 • It developed a method to simulate the SARI process and the SARA process, respectively, and gave likelihood  
482 functions of the SARI model and the SARA model (for the untruncated data), respectively.

483 Our future work will be focused on the derivation of statistical properties of the models.

## 484 Acknowledgements

485 The author is indebted to the reviewers and the editor for their helpful comments.

## 486 References

- 487 [1] L. Doyen, O. Gaudoin, Classes of imperfect repair models based on reduction of failure intensity or virtual age,  
488 Reliability Engineering & System Safety 84 (1) (2004) 45–56.
- 489 [2] S. Wu, P. Scarf, Two new stochastic models of the failure process of a series system, European Journal of  
490 Operational Research 257 (3) (2017) 763–772.
- 491 [3] S. Wu, Superimposed renewal processes in reliability, in: F. Ruggeri (Ed.), Wiley StatsRef: Statistics Reference  
492 Online, Wiley, 2019, pp. 1–12. doi:10.1002/9781118445112.stat08228.
- 493 [4] S. Wu, A failure process model with the exponential smoothing of intensity functions, European Journal of  
494 Operational Research 275 (2) (2019) 502–513.

- 495 [5] Z.-S. Ye, M. Xie, L.-C. Tang, Reliability evaluation of hard disk drive failures based on counting processes,  
496 Reliability Engineering & System Safety 109 (2013) 110–118.
- 497 [6] M. L. Gámiz, B. H. Lindqvist, Nonparametric estimation in trend-renewal processes, Reliability Engineering &  
498 System Safety 145 (2016) 38–46.
- 499 [7] B. Liu, S. Wu, M. Xie, W. Kuo, A condition-based maintenance policy for degrading systems with age-and  
500 state-dependent operating cost, European Journal of Operational Research 263 (3) (2017) 879–887.
- 501 [8] L. Yang, Y. Zhao, R. Peng, X. Ma, Hybrid preventive maintenance of competing failures under random environ-  
502 ment, Reliability Engineering & System Safety 174 (2018) 130–140.
- 503 [9] L. Yang, Z.-s. Ye, C.-G. Lee, S.-f. Yang, R. Peng, A two-phase preventive maintenance policy considering imperfect  
504 repair and postponed replacement, European Journal of Operational Research 274 (3) (2019) 966–977.
- 505 [10] M. Compare, P. Baraldi, I. Bani, E. Zio, D. McDonnell, Industrial equipment reliability estimation: a Bayesian  
506 Weibull regression model with covariate selection, Reliability Engineering & System Safety (2020) 106891.
- 507 [11] L. Brenière, L. Doyen, C. Bérenguer, Virtual age models with time-dependent covariates: A framework for  
508 simulation, parametric inference and quality of estimation, Reliability Engineering & System Safety (2020) 107054.
- 509 [12] B. de Jonge, P. A. Scarf, A review on maintenance optimization, European Journal of Operational Research  
510 (2019).
- 511 [13] P. Kuehn, Approximate analysis of general queuing networks by decomposition, IEEE Transactions on commu-  
512 nications 27 (1) (1979) 113–126.
- 513 [14] W. Whitt, Approximating a point process by a renewal process, i: Two basic methods, Operations Research  
514 30 (1) (1982) 125–147.
- 515 [15] X. Liu, Y. Dijoux, J. Vatn, H. Toftaker, Performance of prognosis indicators for superimposed renewal processes,  
516 Probability in the Engineering and Informational Sciences (2020) 1–24.
- 517 [16] W. Zhang, Y. Tian, L. A. Escobar, W. Q. Meeker, Estimating a parametric component lifetime distribution from  
518 a collection of superimposed renewal processes, Technometrics 59 (2) (2017) 202–214.
- 519 [17] J.-K. Chan, L. Shaw, Modeling repairable systems with failure rates that depend on age and maintenance, IEEE  
520 Transactions on Reliability 42 (4) (1993) 566–571.
- 521 [18] M. A. K. Malik, Reliable preventive maintenance scheduling, AIIE transactions 11 (3) (1979) 221–228.
- 522 [19] M. Kijima, H. Morimura, Y. Suzuki, Periodical replacement problem without assuming minimal repair, European  
523 Journal of Operational Research 37 (2) (1988) 194–203.
- 524 [20] H. Ascher, H. Feingold, Repairable systems reliability: modeling, inference, misconceptions and their causes, M.  
525 Dekker New York, 1984.

- 526 [21] G. Pulcini, Modeling the failure data of a repairable equipment with bathtub type failure intensity, Reliability  
527 Engineering & System Safety 71 (2) (2001) 209–218.
- 528 [22] B. M. Mun, S. J. Bae, P. H. Kvam, A superposed log-linear failure intensity model for repairable artillery systems,  
529 Journal of Quality Technology 45 (1) (2013) 100–115.
- 530 [23] L. Doyen, Asymptotic properties of imperfect repair models and estimation of repair efficiency, Naval Research  
531 Logistics (NRL) 57 (3) (2010) 296–307.
- 532 [24] R. Drenick, The failure law of complex equipment, Journal of the Society for Industrial and Applied Mathematics  
533 8 (4) (1960) 680–690.
- 534 [25] M. Kijima, Some results for repairable systems with general repair, Journal of Applied probability 26 (1) (1989)  
535 89–102.
- 536 [26] S. M. Ross, Stochastic processes, 2nd Edition, John Wiley & Sons New York, 1996.
- 537 [27] K. P. Burnham, D. Anderson, Model selection and multi-model inference: a practical information-theoretic  
538 approach, Springer Science and Business Media, 2002.
- 539 [28] D. M. Louit, R. Pascual, A. K. Jardine, A practical procedure for the selection of time-to-failure models based on  
540 the assessment of trends in maintenance data, Reliability Engineering & System Safety 94 (10) (2009) 1618–1628.
- 541 [29] M. Guida, G. Pulcini, Reliability analysis of mechanical systems with bounded and bathtub shaped intensity  
542 function, IEEE Transactions on Reliability 58 (3) (2009) 432–443.

## 543 Appendix

544 Below gives the proof of Lemma 2.

545 **Proof.** Apparently,  $\epsilon_t \geq -\frac{1}{n} \sum_{k=1}^n \sum_{j=0}^{\min\{m-1, N_{k,t}-1\}} \rho(1-\rho)^j \lambda(T_{k, N_{k,t}-j}) \geq -\frac{1}{n} \sum_{k=1}^n \sum_{j=0}^{m-1} \rho(1-\rho)^j \lambda(T_{k, N_{k,t}-j})$  and  $\epsilon_t \leq$   
546  $\frac{1}{n} \sum_{k=1}^{b_{N_t}} \rho \lambda(T_{N_t-k+1}) + \frac{1}{n} \sum_{k=1}^n \sum_{j=1}^{\min\{\lfloor \frac{N_t}{n} \rfloor - 1, m-1\}} \rho(1-\rho)^j \lambda(T_{N_t-n(j-1)-b_{N_t}-k+1}) \leq \frac{1}{n} \sum_{k=1}^n \rho \lambda(T_{N_t-k+1}) + \frac{1}{n} \sum_{k=1}^n \sum_{j=0}^{m-1} \rho(1-$   
547  $\rho)^j \lambda(T_{N_t-n(j-1)-b_{N_t}-k+1})$ . Note that  $T_{k, N_{k,t}-j} \geq_{\text{st}} T_1$ ,  $T_{N_t-k+1} \geq_{\text{st}} T_1$ , and  $T_{N_t-n(j-1)-b_{N_t}-k+1} \geq_{\text{st}} T_1$ . According  
548 to Definition 2, we have  $E(T_{k, N_{k,t}-j}) \geq E(T_1)$ ,  $E(T_{N_t-k+1}) \geq E(T_1)$ , and  $E(T_{N_t-n(j-1)-b_{N_t}-k+1}) \geq E(T_1)$ . We can  
549 therefore easily obtain that the expectation of  $\epsilon_t$  has the following bounds:

$$550 \quad -\frac{1-\rho^m}{1-\rho} E(\lambda(T_1)) \leq E(\epsilon_t) \leq \rho E(\lambda(T_1)) + \frac{1-\rho^m}{1-\rho} E(\lambda(T_1)) \quad (36)$$

551

552

553 Below gives the proof of Lemma 3.

554 **Proof.** The condition  $j_{k_1} \neq j_{k_2}$  if  $k_1 \neq k_2$  and  $j_{k_1} j_{k_2} > 0$  implies that (1) there is one component renewed, which  
555 has failure rate function  $\lambda_{i_n}(t - T_{i_n, N_t})$ ; and (2) within the others, some may have not renewed since installation time  
556  $t = 0$  and have the same age, and the others may have failed and then renewed at different failure times.

557      Before the first failure, none of the components is replaced. Hence, the failure intensity of the system is  $\frac{1}{n} \sum_{k=1}^n \lambda_k(t)$ .  
558      During the period from the first replacement until the time when the last component installed at time  $t = 0$  is replaced.  
559      ■